FIELD MEASUREMENTS OF IN-SITU EQUIPMENT TRACK PRESSURE AND WORKING PLATFORM DEFORMATION USING EARTH PRESSURE CELLS AND FIBER OPTICS

Peter Faust, Malcolm Drilling Company Inc., USA, pfaust@malcolmdrilling.com
Peter Hubbard, UC Berkeley, USA, phubbard@berkeley.edu
Kenichi Soga, UC Berkeley, USA, soga@berkeley.edu

ABSTRACT

The European Federation of Foundation Contractors (EFFC) and The Deep Foundations Institute (DFI) have set up a task group to compile a Guide for Working Platforms. The first edition of this Guide has been published in January 2020. The aim of the Guide is to provide reliable methods for design, testing and verification of working platforms for construction equipment, especially in the deep foundation industry where track loads can be excessive due to the nature of its operations. The Guide has identified areas where knowledge is limited. Actual track pressure and its distribution along the length of the tracks is still not well researched. Current recommendation provided in EN 16228-1 are believed to be overly simplified and may lead to conservative requirements for working platform thickness.

This paper presents results of a series of field tests where the actual track pressure of a large drilling rig during operation was measured in real time together with the deformation of the working platform. Embedded, distributed fiber optic sensing (DFOS) at different depths throughout the platform allowed for a three-dimensional evaluation of the platform deformation throughout the entire operation. Results will help to develop more reliable recommendations for future safety requirements of working platforms for deep foundation equipment.

Keywords: Working Platform, Track Pressure, Earth Pressure Cells, Distributed Fiber Optic Sensing (DFOS), Distributed Strain Sensing (DSS), BRE, EN 16228-1

INTRODUCTION

Large foundation equipment like pile drilling or driving machines can exert over 800 kPa [16,708 psf] track pressure onto the subsurface during their operation. If this working platform is comprised of soft cohesive of loose non-cohesive soil, the need for improvement to stabilize the subsurface or the addition of load spreading steel plates or crane mats (also called timber mats) is commonly required. Cost to improve the subsurface by means of densification or the addition of lime or cement can be a substantial add to the overall construction cost. Utilizing crane mats is often the only alternative when working in coastal environments where thick layers of non-cohesive soil layers are predominant or cannot be stabilized. Working off crane mats will greatly reduce the productivity and therefore increase overall construction cost.

While several publications provide guidance on how crane mats distribute loads, very little information is available about the benefits of steel plates. To the knowledge of the authors no field tests measuring and comparing the actual ground bearing pressure on native soil, steel plates and crane mats have been performed. This paper summarizes findings from 3 different field tests utilizing a large drilling rig placed on native soil alone, steel plates and crane mats while pulling with up to 90 tons on a pre-installed ground anchor. Pressure cell as well as fiber optic sensors were placed in the ground to measure pressure and deformation as the load was applied in stages.

While results will help compare the benefits of using crane mats or steel plates to provide stable and safe working conditions for deep foundation equipment, the measured pressure distribution along the machines tracks deviated surprisingly from commonly used theoretical calculation methods as used in EN 16228-1 or the BRE guideline.

TEST SET UP

To be able to achieve controllable machine operating conditions, it was decided not to measure track pressures during actual pile drilling, but rather to apply the pulling force to one pre-installed tie-down anchor. One Bauer BG46 drilling rig was used for all 3 test configurations as shown in Figure 1. The machine can apply over 100 tons- of pull force using both main winches. The onboard data acquisition system B-Tronic was utilized to monitor the applied winch force for each load cycle.

Figure 1. BG46 drilling machine with 3 different testing configurations

The first test series was performed on 300 mm [12 in] thick crane mats followed by 25 mm [1 in] thick steel plates before the bare native soil was loaded. This sequence was chosen to minimize the influence of pre-loading and potentially densifying the soil of the work platform embedding the instruments.

For safety reasons only a maximum of 90 tons of pulling force was applied for each test.

SUBSURFACE CONDITIONS

Site conditions were typical for coastal areas where very soft non-cohesive soils are predominantly found very close to the working surface. The test location had about 3-5 m [10-15 ft] of man-made fill material over a 5 m [15 ft] layer of very soft clay with shear strength of less than 50 kPa [1,000 psf] . Very high operating loads were expected since 1.2 m [4 ft] Continuous Flight Auger Piles had to be installed on site. It was therefore decided to remove the upper 1 m [3.5 ft] fill and place an additional 450 mm [18 in] layer of cemented soil below an upper layer of 600 mm [24 in] well compacted, medium coarse aggregate for surface water containment.

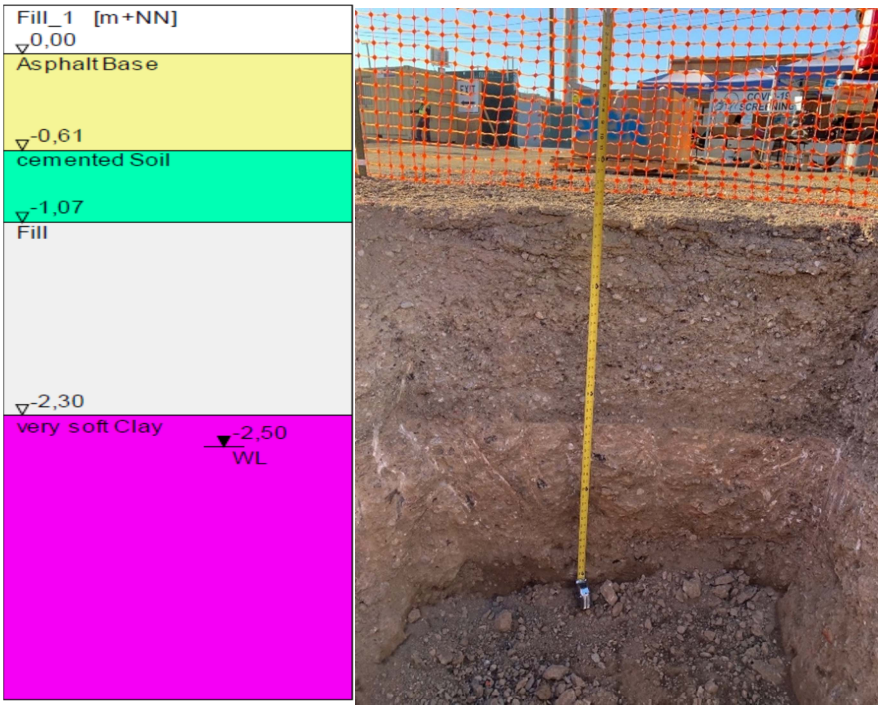

Figure 2. Subsurface conditions with picture of cement treated soil layer below top layer of aggregate (asphalt) base

INSTRUMENTATION

Geokon Earth Pressure cells were used underneath one track to measure the earth pressure induced by the track loading. Earth pressure cells are constructed by two stainless steel plates welded together around their periphery and separated by a narrow gap filled with hydraulic fluid. External pressure squeezes the two plates together creating an equal pressure in the internal fluid. A length of stainless-steel tubing connects the fluid filled cavity to a pressure transducer that converts the fluid pressure to an electric signal transmitted by cable to the readout location. Model 4815 is a special cell that effectively reduces the severity of point loading when used in granular materials. The modification uses two thick plates welded together at a flexible hinge that helps provide more uniform pressure distribution.

In addition, vertical fiber optic cables were embedded underneath the other track and in two horizontal loops across both tracks. Distributed fiber optic sensing (DFOS) is a group of sensing technologies that measure spatially continuous information about an optical fiber. DFOS can measure strain and temperature along an optical fiber ranging from a few meters to tens of kilometers in length. The interrogation method used to examine the sensing fiber determines the maximum sensing distance, spatial resolution, and readout interval (Soga and Luo 2018). DFOS has been widely applied in the field of civil engineering to monitor infrastructure including tunnels, retaining walls, deep foundations, and

bridges (Di Murro et al. 2019; Mohamad et al. 2011; Pelecanos et al. 2018; Alexakis et al. 2021). In this work, the technique of optical frequency domain reflectometry (OFDR) was employed using a Luna Innovations ODiSI 6000 interrogator unit with a spatial resolution and readout interval of 0.6mm and a maximum sensing length of 50m (Luna Innovations, 2020).

DFOS was installed within the working platform to monitor the strain caused by the drill rig when it pulled on a tie-down with different amounts of force. It was desired to localize the deformation within the platform to describe the geometric loading pattern underneath the rig's tracks.

To effectively measure the strain using DFOS, a cable designed for this purpose must be used. The strain must be transferred from the platform material to the cable, and then from the cable's outer sheath to the fiber optic core. To achieve transfer from the sheath to the core a heavily tested and field deployed cable manufactured by Nanzee sensing was selected (Zhang et al. 2019). The cross-section is shown in Figure 3. This cable is comprised of a stiff polyethylene sheath enclosing six steel braids tightly woven around a tightly buffered single mode optical fiber.

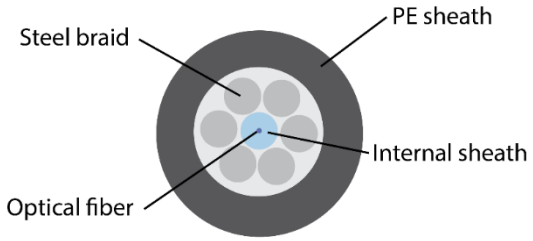

Figure 3. Cross-section schematic of the field deployed fiber optic cable for sensing strain in the working platform

INSTRUMENTATION LAYOUT

A total of 7 earth pressure cells were installed in about 300 mm [12 in] depth from the working surface. The cells were placed in the excavation on native ground without embedment in an additional grout bed. The excavation was backfilled with the previously excavated material and carefully compacted with a small vibro plate by adding small amounts of water. No further testing of compaction level was performed. All cells were connected to a Geokon datalogger to collect the pressure data.

Nine separate DFOS cables were deployed and interrogated on different channels during the load test. The alignment of the cables is shown in Figure 4. Seven of the cables were installed vertically while two were installed horizontally. The seven vertical fibers were installed by drilling 100 mm [4 inch] diameter boreholes to the desired maximum measurement depth of 7.6 m [25 feet] below grade and then lowering the cable within the hole, attached to a 12.5 mm [0.5 inch] Sch40 PVC tremie pipe. The holes were then grouted with an instrumentation cement-bentonite grout with an approximate shear strength of 345 kPa [50 psi]. After grouting the fibers were pre-tensioned manually with 220 N [50 lbs] of tensile force applied at the surface. After the grout mix cured for 48 hours, the pretension was released, and the platform was excavated down 280 mm [1 foot] underneath where the tracks would eventually sit. This allowed for the placement of the horizontal cables, which were laid straight but loosely in the configuration showed in Figure 5.

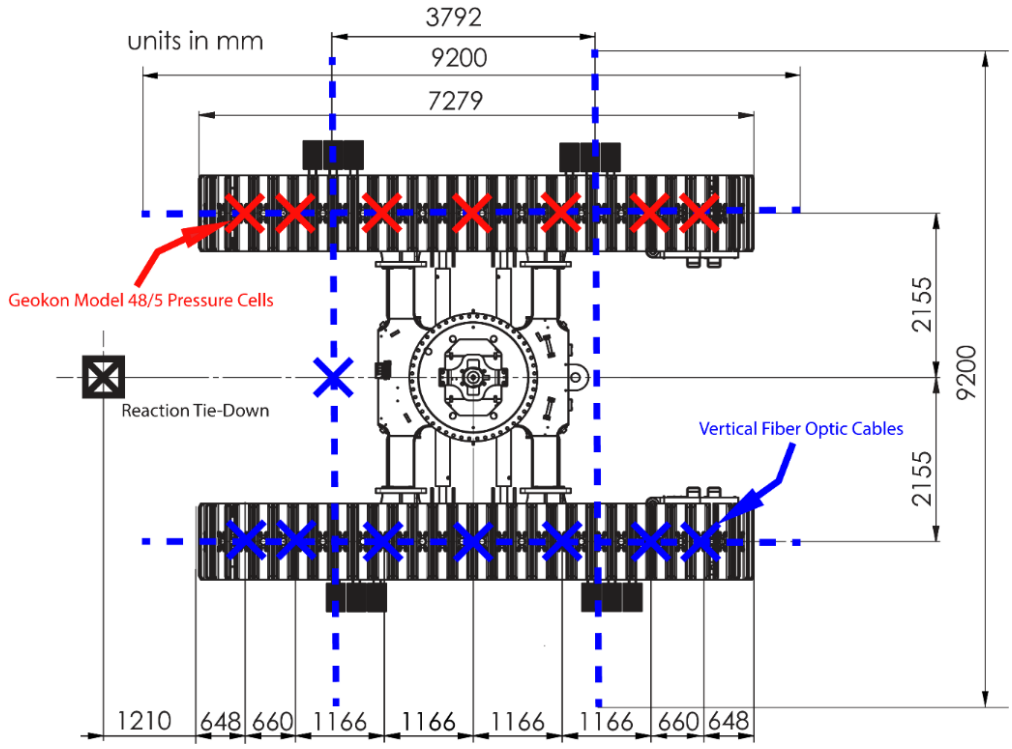

Figure 4. Overview of the Cable and Cell Layout

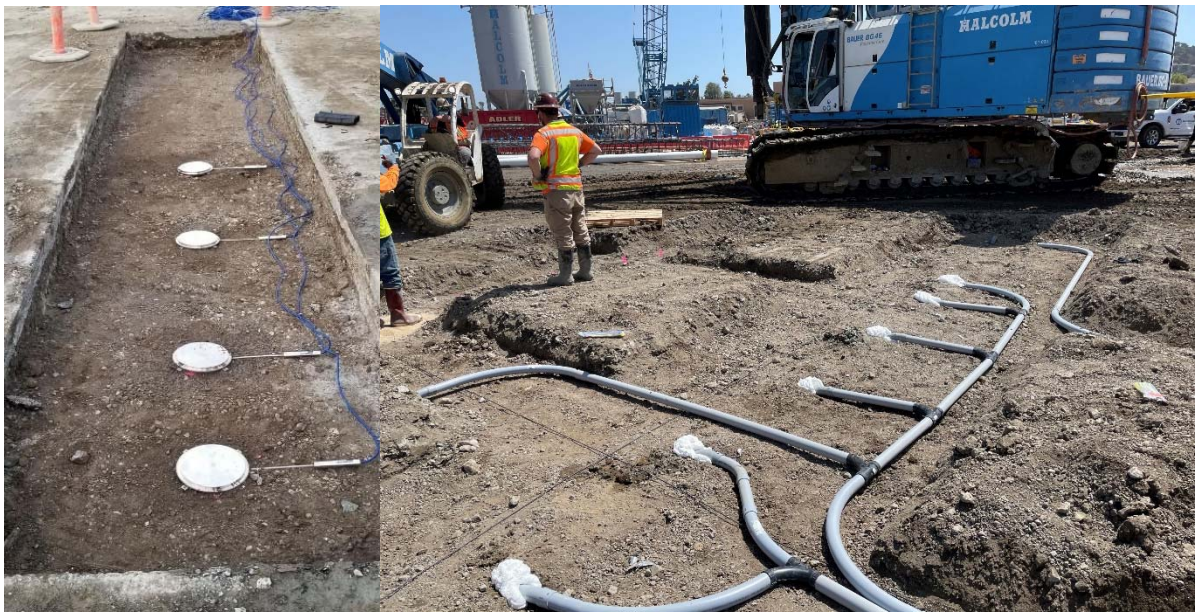

Figure 5. Cell and cable placement

For each testing configuration the rig was walked into place, the rotary of the machine was attached to the tie-down with chains and load was applied in 10 tons increments. Each load step was held for 5 minutes for sensor readings to take place.

EARTH PRESSURE MEASUREMENTS

Each test started by tracking the machine onto the working pad. The first pull test was performed on crane mats, the second test on steel plates followed by the last test on native ground.

Figure 6 shows the measured pressure before pulling force was applied to the tie-down. While pressure distribution of the last configuration (ground) demonstrate that the dead weight of the machine is well aligned with its center of gravity, the first two measurement series show almost no or slight negative pressure. There is no obvious explanation for this phenomenon since all cells were calibrated and functioned well throughout the entire test. As soon as pull load was applied, pressure cells indicated pressure levels similar to measurement in Figure 7. Final measurements after all pull tests were completed, confirmed initial measurement as shown in Figure 10.

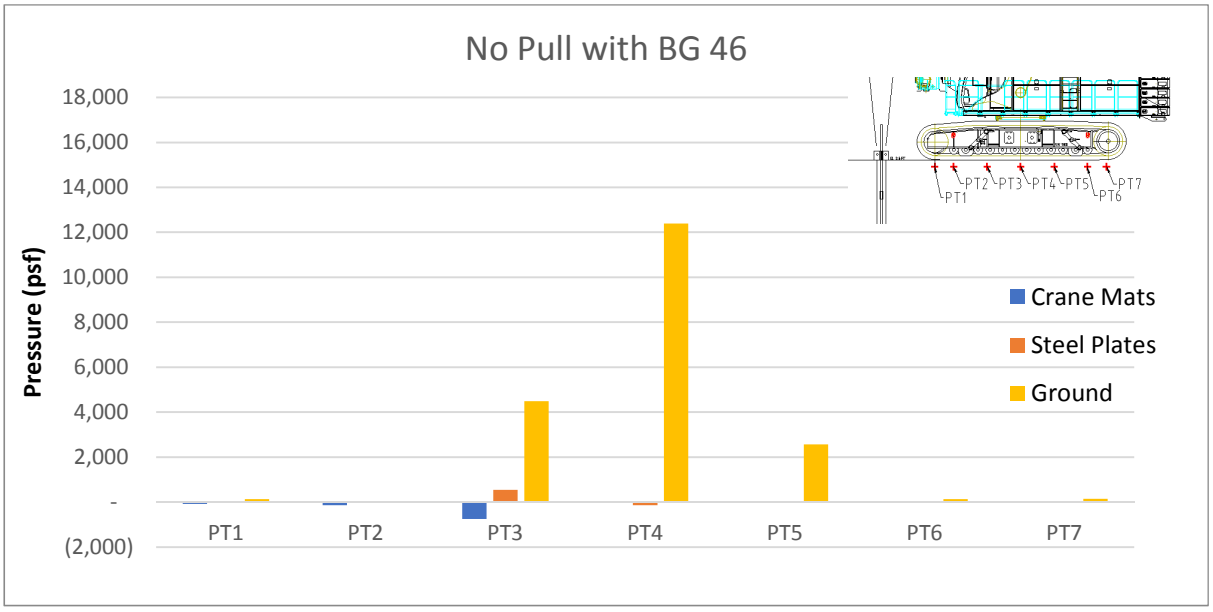

Figure 6. Earth pressure measurement with machine dead weight only

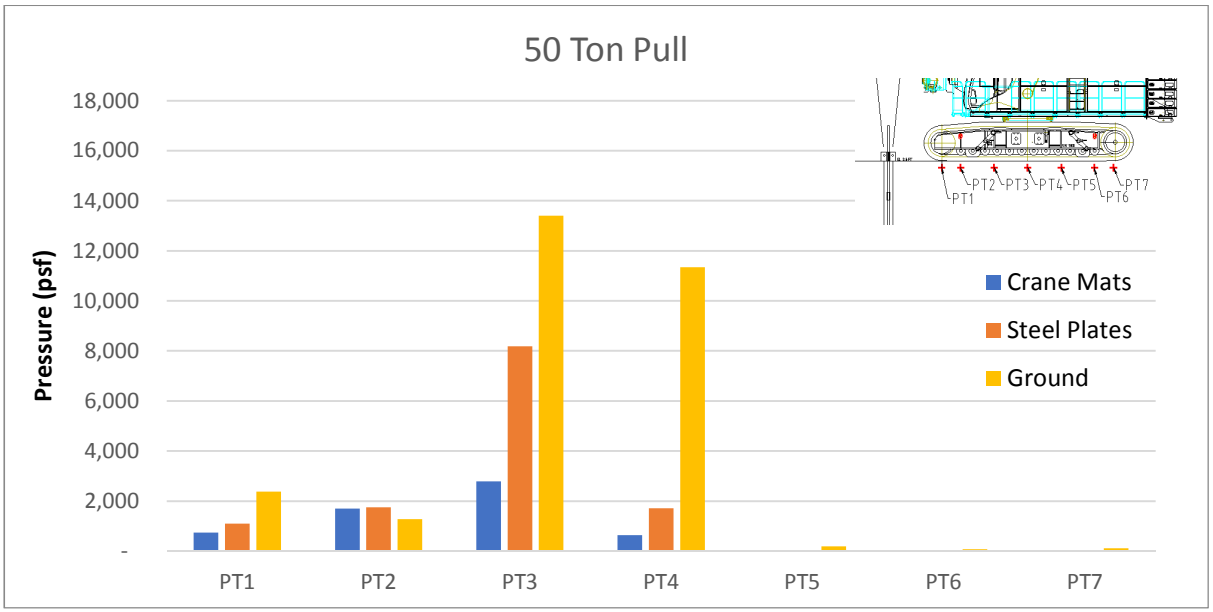

Figure 7. Earth pressure measurement at 50 ton pull

As the load is increased (Figure 8), the center of gravity of the drill rig is slowly moving forward and pressure underneath the front half of the tracks increase, while the rear of the machine is almost not inducing any load into the ground. It can be observed that for all three test configurations (mats, steel plates and ground) the highest pressures are still recorded towards the center of the machine and not at the front of its tracks.

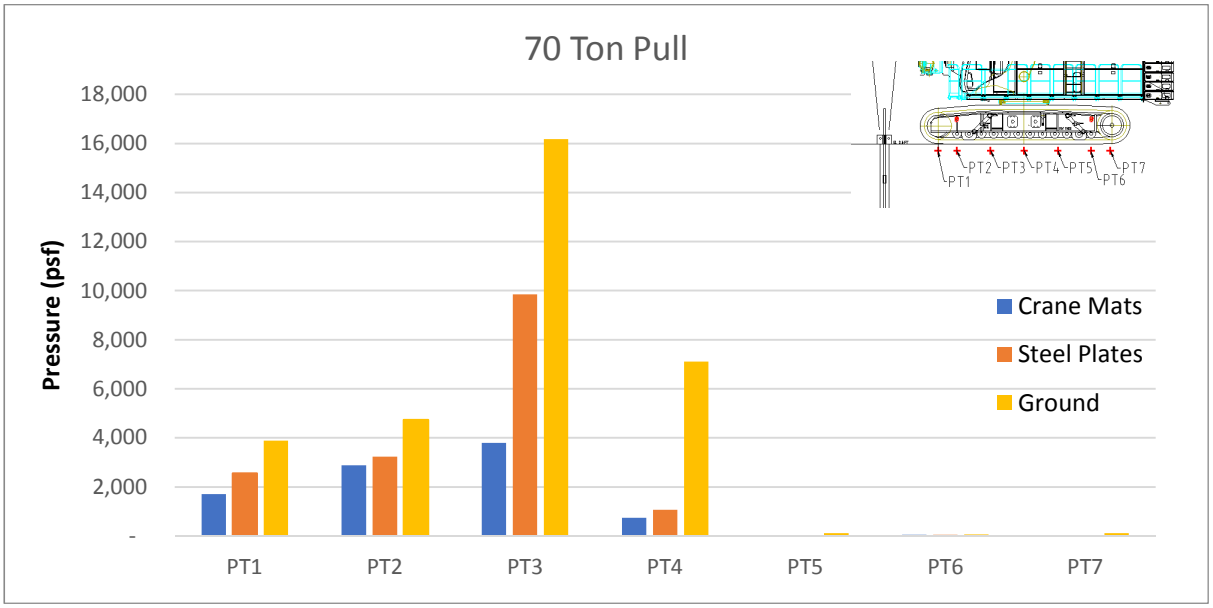

Figure 8. Earth pressure measurement at 70 ton pull

The maximum applied pull force of 90 tons is still resulting in peak pressures been concentrated around the middle of the machine and not at the front of its tracks. All 3 test configurations correlate well, despite that the size of utilized crane mats was not the same as for the steel plates and may therefore contributed to minor irregularities in pressure distribution. It can clearly be seen that only crane mats distribute the load consistently between the front and the middle of the machine, while steel plates do not achieve the same. Steel plates remarkably reduce the peak pressure but cannot substitute crane mats in their pressure distribution function.

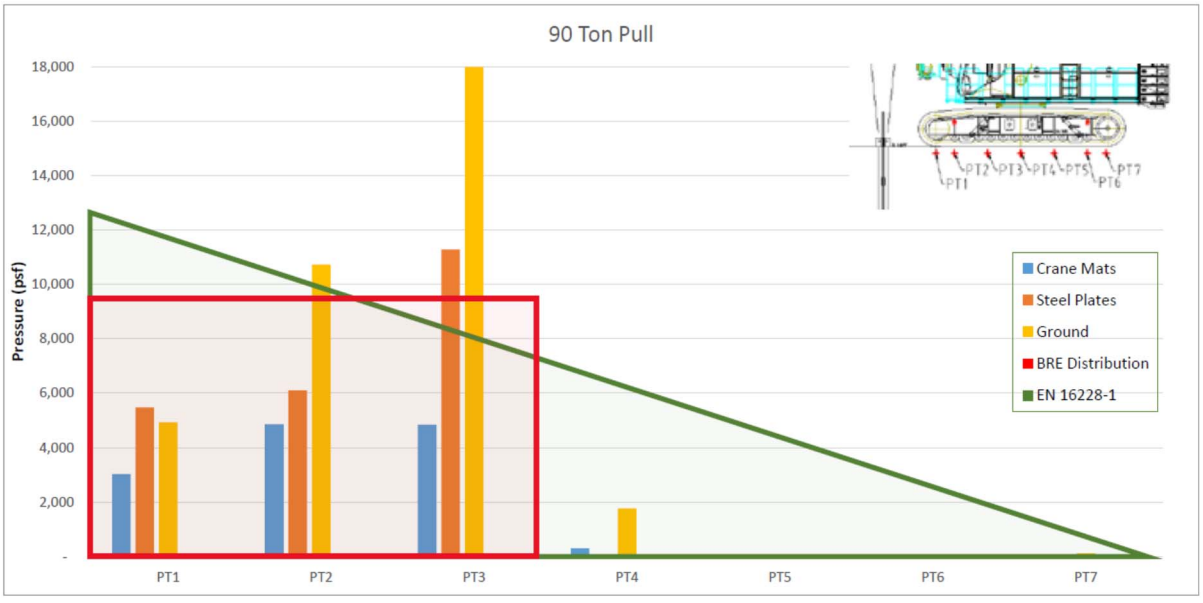

Figure 9. Earth pressure measurement at 90 ton pull

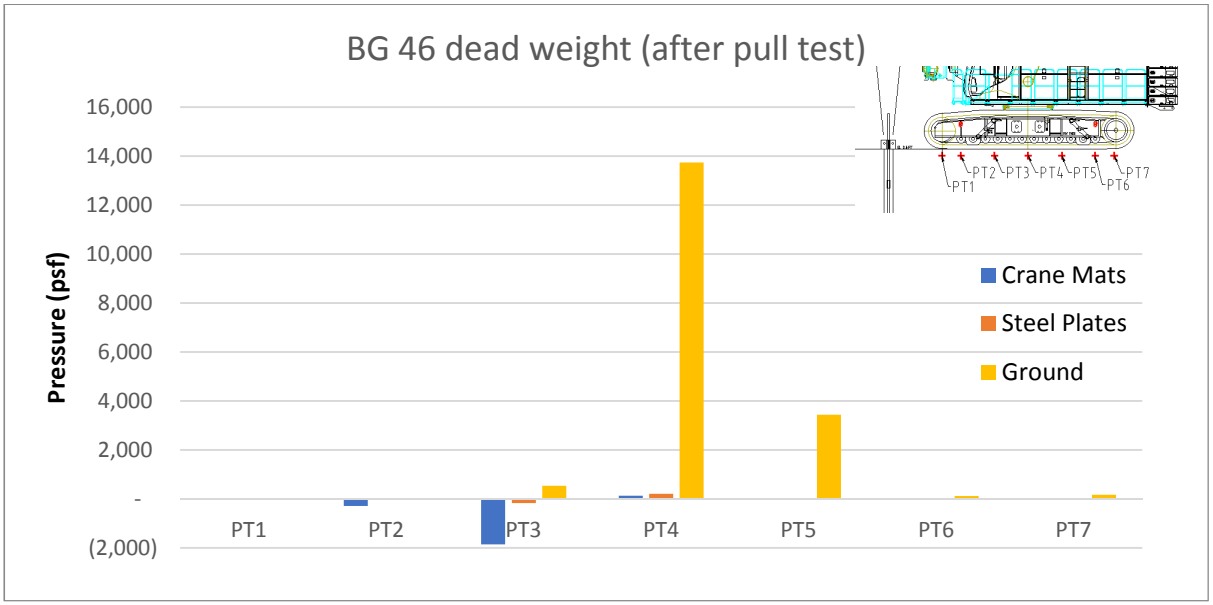

Figure 10. Earth pressure measurement after pull tests were completed

Since earth pressure cells are made from steel and are therefore much stiffer than the surrounding soil, load concentrations in selective cells are possible. Three separate tests with only pressure measurements to investigate the influence of different backfill types were performed. For Backfill #1 and #3, the previously excavated working platform material was utilized with similar moisture contents. The material was placed in one layer and compacted using a small vibro plate compactor. For Backfill #2 a dry coarse sand was utilized, and additional compaction was minimal. No additional in-Situ material or compaction tests were performed. Figure 11 shows the difference in pressure measurements between these 3 different backfill materials. The extreme deviation of PT2 can be attributed to the very loose fill material, which resulted in a severe stress concentration around this cell since measurements for this load level 50 tons) are well above anything else recording during the other pull test series with forces of up to 90 tons.

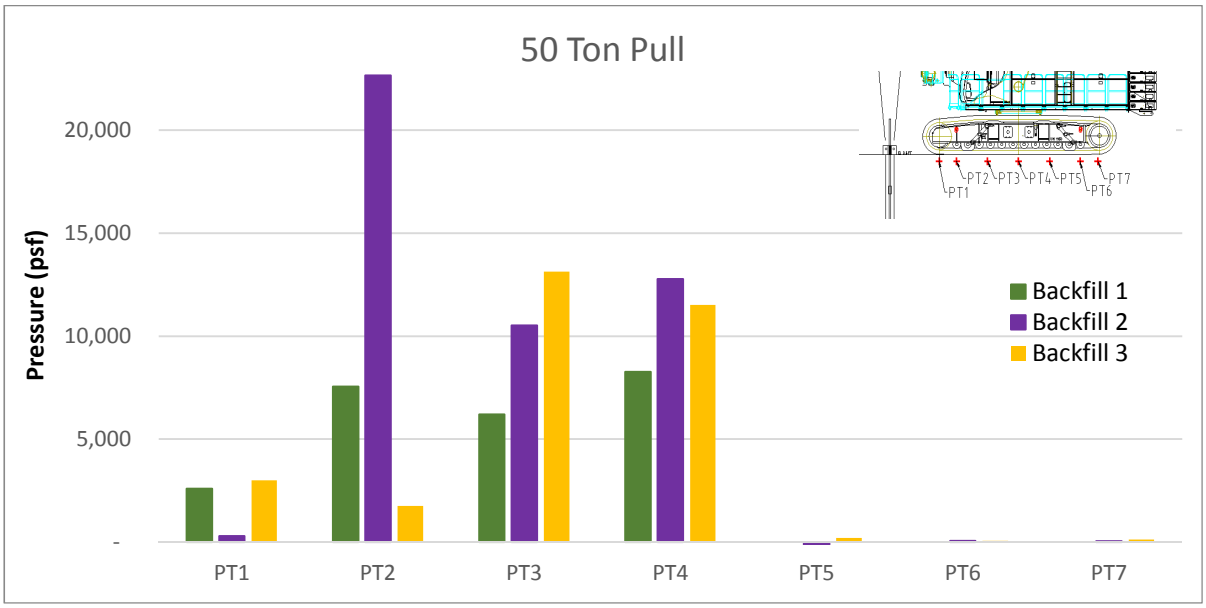

Figure 11. Earth pressure measurement on 3 different backfill materials

VERTICAL STRAIN AND DISPLACEMENT MEASUREMENTS

Strain measurements made with OFDR technology are relative to a baseline reading. A baseline can be selected before or after the measurements are made, making it convenient to compare different times during testing. For each different surface protection scenario, vertical strain measurements are shown relative to the ground condition before the drill rig was placed on top of the sensors for each respective test.

The vertical measurements were made at the discrete locations of the vertical optical fibers in the platform and subsurface. Seven of the vertical sensing fibers were oriented in a line underneath the left track of the drill rig. These measurements were used to interpolate a 2D image of the strain field between the fibers using a non-linear interpolation scheme.

After creation of the 2D strain image, each vertical column of interpolated measurements (pixels) was integrated numerically from bottom to top. This integration is common for fiber optic strain measurements to calculate the displacement along the fiber (Pelecanos et al. 2016). The displacement image can then be displayed much like the strain image.

In addition to the 2D strain images from measurements made underneath a track, one additional vertical fiber optic strain sensor was placed in the center, between the tracks of the drill rig. The data from this sensing line is displayed on its own.

Under-track measurements

The strain and displacement images for each case under maximum loading are shown in Figure 12. The top row of images corresponds to the strain while the bottom row of images corresponds to the displacements determined by integrating vertically along each column of strain values.

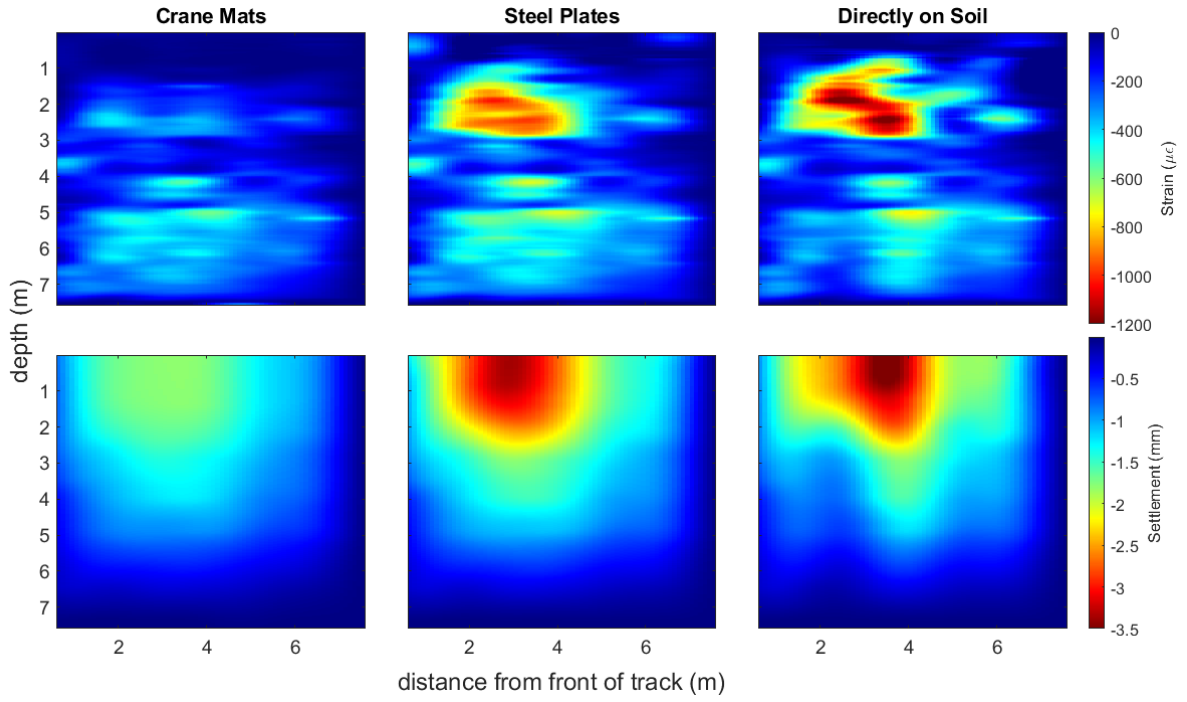

Figure 12. Strain and displacement images determined by DFOS underneath the left track of the drill rig during 70 tons of pulling force.

The magnitudes of strain and displacement vary for each case as well as the location of the maximum displacement horizontally underneath the track. For the crane mats, the maximum strain value is located

at 4 m [12 feet] towards the rear from the front of the track and 5 m [15 feet] deep into the platform with a value of 580με. The steel plates cause a maximum strain location of 2.5 m [8 feet] from the front of the track at a depth of 1.8 m [6 feet] and a value of 1030με. This is the same location of the maximum strain when the rig is directly on the soil, though the value is higher at 1275με.

The location of maximum displacement shifts from 3.8 m [12 feet] from the front of the track with the crane mats to 3 m [10 feet] from the front for the steel plates and 3.5 m [11.5 feet] for the case when the rig was directly on the soil. More importantly, the shape of the vertical displacement distribution varies widely for the three cases. This is shown in Figure 13.

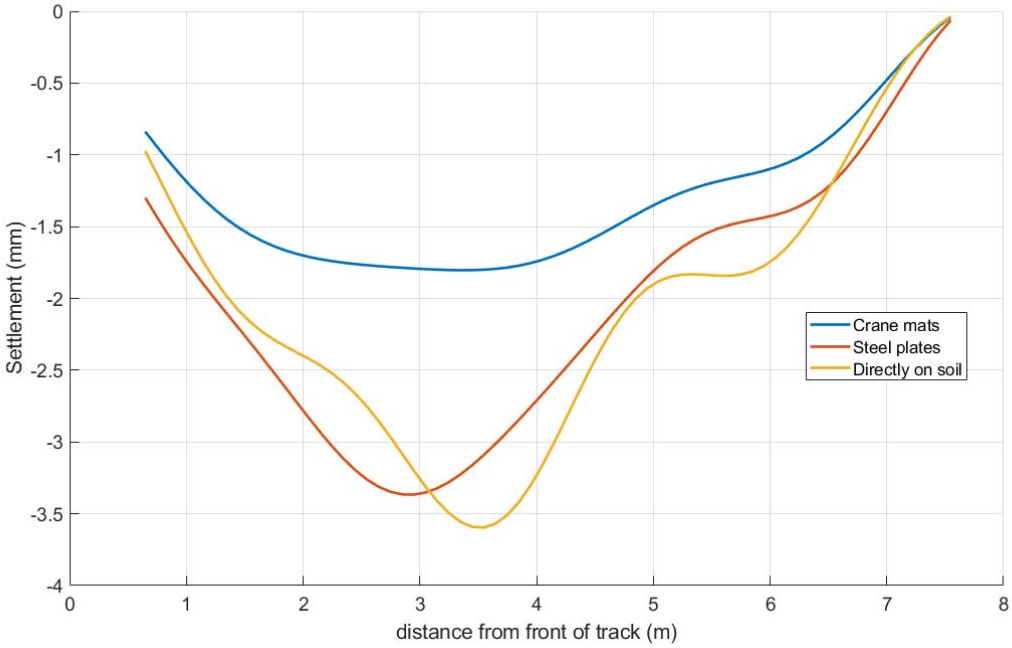

Figure 13. Settlement distribution underneath the left track during the 70 tons- pull with three different test configurations

Figure 13 shows that using the crane mats results in a vertical deformation that does not have a clear maximum. The steel plates exhibit a clear maximum value -3.4 mm [-0.13 inch] but still has a more gradual distribution than the case when the rig is directly on the soil. In this case there is a sharp maximum at 3.5 m [11.5 feet] from the front of the track with a value of -3.6 mm [-0.14 inch].

The accumulation of strain and displacement during the progression of loading when the rig was directly on the native soil is shown in Figure 14 This data demonstrates that before the rig begins pulling the weight is distributed towards the rear of the tracks. The weight shifts forwards as pulling increases. However, the load is never highest at the front of the tracks as assumed by a trapezoidal load distribution. Instead, the maximum strain and ground displacement is experienced about one-third of the track length behind the toe of the rig.

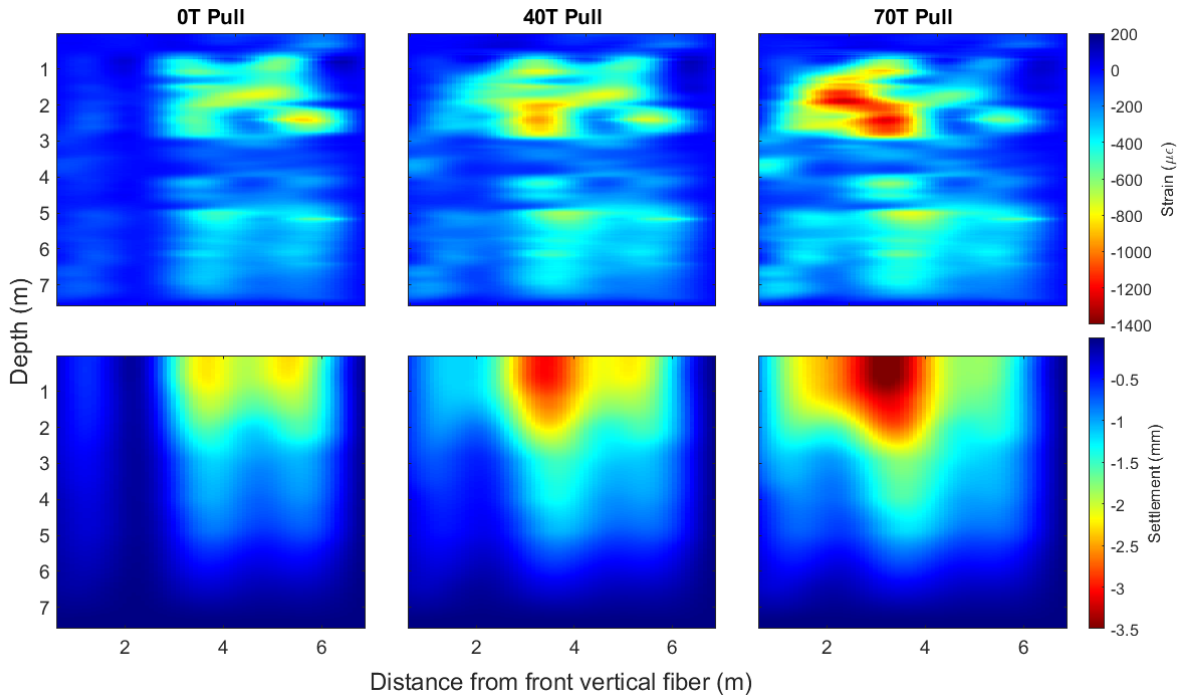

Figure 14. Strain and displacement images determined by DFOS underneath the left track of the drill rig on the native ground during 0 tons, 40 tons and 70 tons of pulling force being applied

Vertical Measurements between the tracks

As shown in Figure 4, a single vertical fiber was placed in between the tracks 1.90 m [6 feet] in front of the center of the drill rig. The strain data from this sensing line is shown in Figure 15. The strain data was integrated vertically to get the displacement profile is shown in Figure 16.

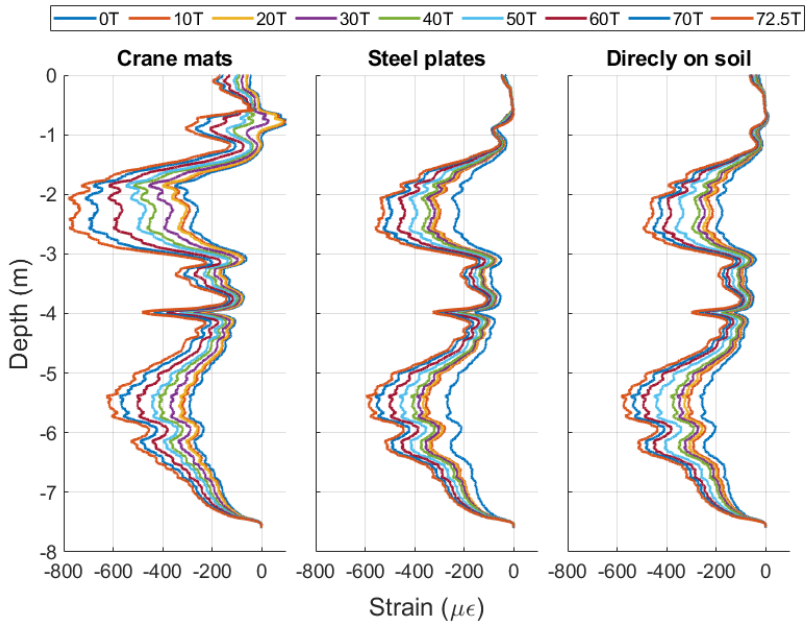

Figure 15. Vertical strain profiles between the tracks of the drill rig for each loading step and test configuration.

The strain data shows that the crane mats cause a larger strain in the upper 3 m [9.8 feet] of the platform in between the tracks than the steel plates or the soil alone. In addition, the strain profiles below 4 m [12 feet] are similar in both geometry and magnitude for all three cases.

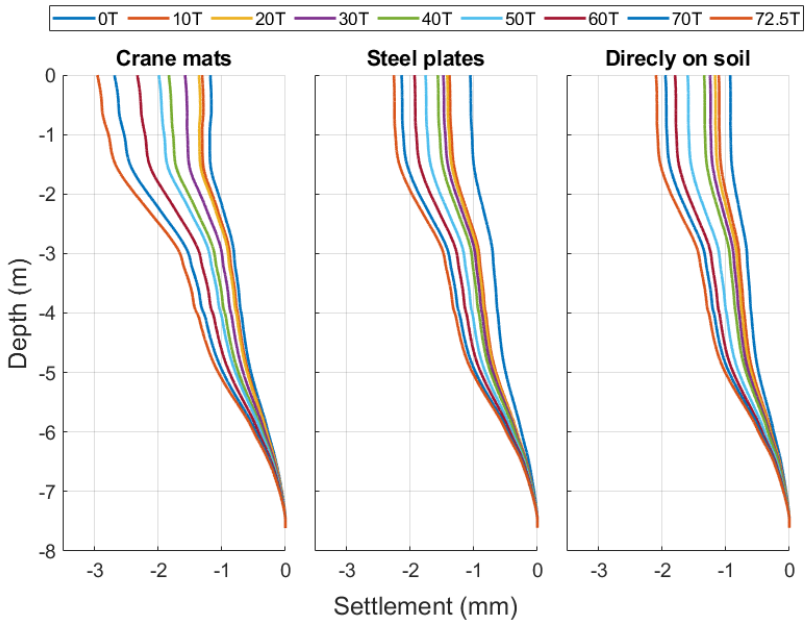

Figure 16. Vertical displacement profiles between the tracks of the drill rig for each loading step and test configuration.

The displacement data shows that the magnitude of settlement between the tracks is greatest when the crane mats are used. The compressive deformation is concentrated between -2 and -3 m [6.5 and 9.8 ft] below the ground surface. Since no settlement is measured in the top 1m for the steel plate and directly on soil tests, it is assumed that the coupling between the soil and cable at the near surface was poor. Decoupling in the top 1m may have occurred during the crane mat test which was conducted first.

Horizontal measurements along the tracks

The horizontal strain measurements made by the cables along the tracks in Figure 4 indicate how the load is distributed during each test case. These data sets are shown relative to the first load step. The horizontal strain that occurred when the crane mats were used is shown in Figure 17. There is a distinct zone of compression towards the front of the track centered at about 1 m [3 feet]from the front of the track. There is also a zone of relative tension that is centered at about 5 m [15 feet] from the front of the track, indicating that the load is transferred to the soil predominantly in the front 3 m [10 feet] of track contact with the crane mats.

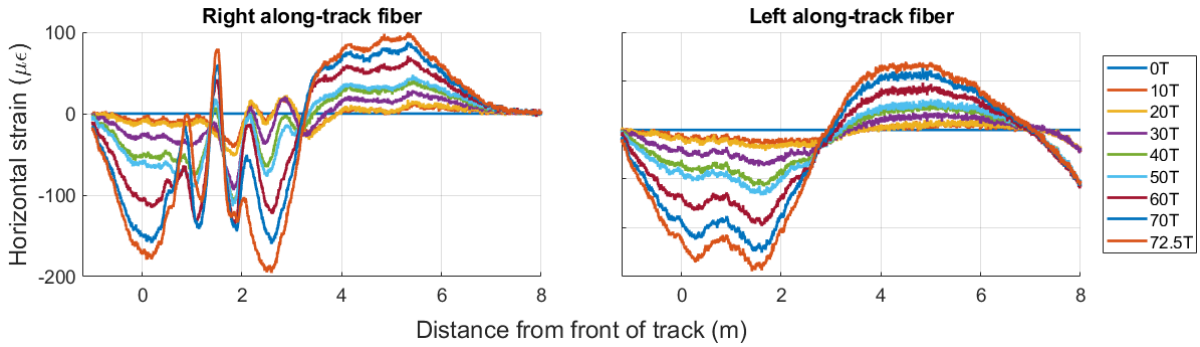

Figure 17. Horizontal strain data measured underneath the tracks in the direction of the tracks when the crane mats are used.

The horizontal strain data when the steel plates were used indicates a similar trend as the crane mats but is more variable due to a less effective distribution of the rig's weight and the force generated by pulling on the tie-down. Figure 18 shows this data. The magnitude of the strain is much higher than the strain seen during use of the crane mats. The major peaks in the horizontal strain are still towards the front of the track but have slightly shifted towards the rear of the rig. Most of the strain occurs in the front 4 m [12 feet] of the tracks.

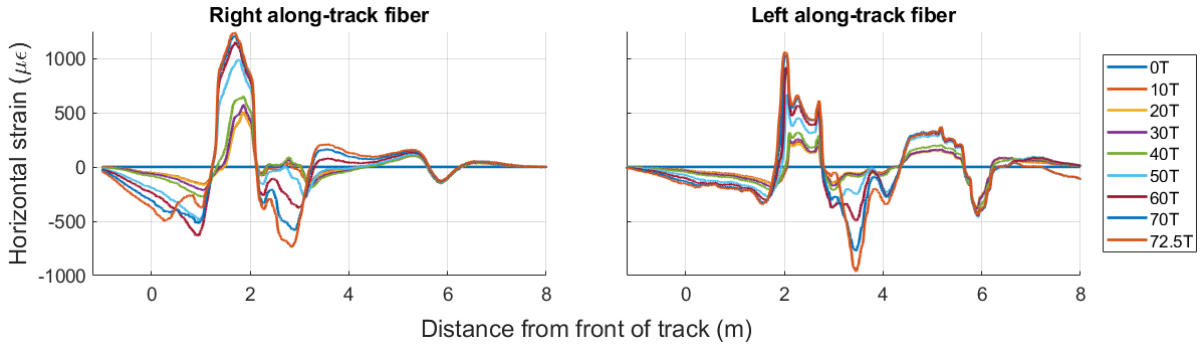

Figure 18. Horizontal strain data measured underneath the tracks in the direction of the tracks when the steel plates are used.

The horizontal strain data when the drill rig was directly on the soil is shown in Figure 19. The magnitude of the horizontal strain is less than during the use of the steel plates. This may be explained by permanent compaction of the soil during the previous tests resulting in a stiffer shallow platform material and/or localized shearing in the soil at the shallow depths causing decoupling between the cable and the sandy fill material. The data from the left track still shows a similar trend to the other conditions with a zone of compression in the front 4 m [12 feet] centered at about 2.2 m [7 feet] and a zone of relative tension toward the rear of the track centered at about 4.3 m [14 feet].

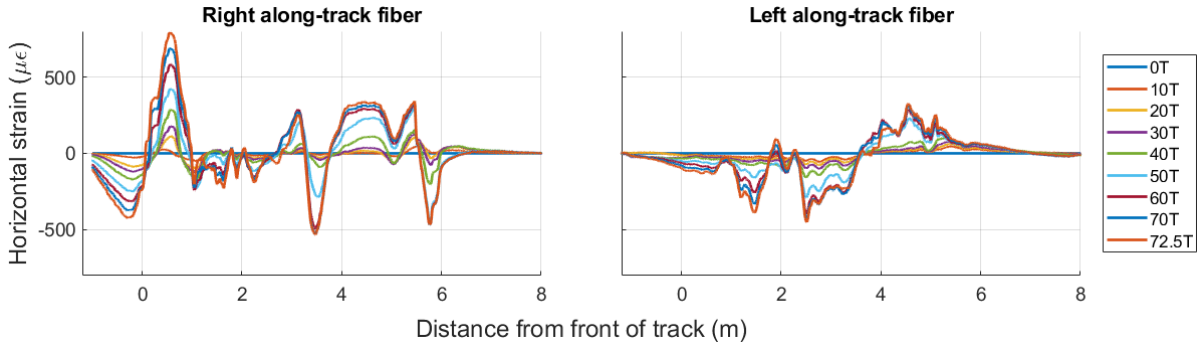

Figure 19. Horizontal strain data measured underneath the tracks in the direction of the tracks when the rig is directly on the soil.

DISCUSSION OF DATA

The earth pressure cell readings and the vertical strain data from beneath the left track and between the tracks suggest the following:

- Fiber optics have confirmed the magnitude and overall distribution of track pressure readings using earth pressure cells and are therefore a very helpful tool to measure actual track pressure of drilling rigs for various loading conditions.
- The maximum track pressure does not necessarily occur at the front of the tracks. It is rather a function of loading level and machine weight distribution between front and back. Subsurface conditions do also influence the pressure distribution.
- The pressure distribution underneath the drill rig is not trapezoid as assumed by most theoretical design models.
- Crane mats distribute the load very effectively as evidenced by both the measurements made underneath the track and in between the tracks. The location between the tracks experienced the maximum strain and vertical displacement during the use of the crane mats over the use of steel plates or when the drill rig was on the native soil alone
- Steel plates provide no significant improved pressure distribution compared to native soil. They will only bridge small, localized inconsistencies in the work platform.
- The influence of crane mats or steel plates is not significantly seen after 4 m [12 feet] depth into the working platform. The strain below 4 m [12 feet] is about the same indicating that the load is evenly distributed by this depth.

CONCLUSIONS

Exact track pressure measurements for foundation equipment or cranes using earth pressure cells are difficult to accomplish and depend largely on compaction levels of the surrounding soil. Localized pressure peaks are contributed to stress concentrations within the cell when surrounded by much softer soil. More research is needed to investigate actual pressure distribution under modern, very heavy machines which can apply very high loads onto their working platform for certain operations like the installation of CFA piles.

Available design models to calculate track pressure typically utilize drastically simplified pressure distributions models as for rigid shallow foundations. These models require adjustments to reflect the actual track pressure conditions and may also have to include consideration of the subsurface stiffness.

Strain measurements using DFOS technology are a useful tool to confirm magnitude and distribution of earth pressure readings. Installed in a vertical arrangement right underneath the machine tracks, they can provide vertical settlements of a working platform under heavy loading conditions in real time. Furthermore, several vertically grouted fiber optic strain sensors provide a way to visualize a 2D cross-section of the strain and displacement profile.

The presented field test confirms previous assumptions that investigation depth for any work platform design should exceed 4 m [12 feet] and extend preferably to 5 m [15 feet] regardless of if crane mats or steel plates are used.

REFERENCES

Alexakis C, Lau FD, DeJong MJ. (2021) Fiber Optic Sensing of Aging Railway Infrastructure enhanced with Statistical Shape Analysis, *Journal of Civil Structural Health Monitoring*, 11, 49-67. DOI: 10.1007/s13349-020-00437-w

BR 470 (2004) Working platforms for tracked plant: good practice guide to the design, installation, maintenance and repair of ground-supported working platforms, BRE Bookshop

Di Murro V, Pelecanos L, Soga K, Kechavarzi C, Morton RF and Scibile L. (2019) Long-term deformation monitoring of CERN concrete-lined tunnels using distributed fibre-optic sensing. Geotechnical Engineering Journal of the SEAGS & AGSSEA, 50(2), pp.1-7. http://seags.ait.asia/journals/32613-seags-agssea-journal-june-2019/

Duerr D, Mobile Crane Support Handbook (2019), Levare Press, Inc.

EFFC-DFI Guide to Working Platforms (2020)

EN 16228-1 (2014) Drilling and foundation equipment. Beuth Publishing Company

Luna Innovations. (2020) ODiSI 6000 Series Optical Distributed Sensor Interrogators.

Mohamad H, Soga K and Pellow A. (2011) Performance Monitoring of a Secant Piled Wall Using Distributed Fibre Optic Strain Sensing, *Journal of Geotechnical and Geoenvironmental Engineering*, American Society of Civil Engineers, 137(12), pp. 1236-1243, DOI: 10.1061/(ASCE)GT.1943-5606.0000543.

Moorman C, (2019) Tragschichten fuer Arbeitsplattformen, FVB

Pelecanos L, Soga K, Elshafie M, de Battista N, Kechavarzi C, Gue CY, Ouyang Y and Seo H. (2018) Distributed Fibre Optic Sensing of Axially Loaded Bored Piles, *Journal of Geotechnical and Geoenvironmental Engineering*, American Society of Civil Engineers, 144(3), pp. 16. doi: 10.1061/(ASCE) GT.1943-5606.

Soga K, & Luo L. (2018). Distributed fiber optics sensors for civil engineering infrastructure sensing. *Journal of Structural Integrity and Maintenance, 3*(1), 1-21. DOI:10.1080/24705314.2018.1426138

Topolnicki M, Waeger J, Schweizer S, Koller A, Brzozwski T, Soltys G, Field test verification of ground bearing pressure (2021) *Technical Paper in Ground Engineering Magazine*

Zhang C, Shi B, & Soga K. (2019). Distributed Fiber Optic Sensing of Land Deformation: Methods and Case Studies. In *Selected papers from sessions of the Eighth International Conference on Case Histories in Geotechnical Engineering*, Reston, VA: ASCE. DOI: 10.1061/9780784482131